



INFLUENCE OF AXIAL FLOW COMPRESSORS FUNDAMENTAL DIMENSIONLESS PARAMETERS FOR ROTATING STALL AND SURGE

Shaaban I. Ahmed ^a, M. G. Higazy ^b, Ahmed Y. Sayed ^c and Emad A. SAYED ^d

^a Department of Engineering Mathematics and Physics, Faculty of Engineering, Modern University for technology and information, Cairo, Egypt

^b Department of Mechanical Engineering, Faculty of Engineering Shoubra, Benha University, Now Dean of Alsalam Higher institute of engineering and technology, Cairo, Egypt

^c Department of Engineering Mathematics and Physics, Faculty of Engineering El-Matara, Helwan University, Cairo, Egypt

^d Department of Engineering Mathematics and Physics, Faculty of Engineering El-Matara, Helwan University, Cairo, Egypt

Abstract. Numerical solution for the surge and rotating stall in axial flow compressor is considered. The main objective of this study is to explain the unsteady behavior of the rotating stall and surge phenomena to increase the value of stability for the axial compressor. The performance of the compressor will be improved significantly by decreasing the effect of stall and surge for axial flow compressor. The results are verified as compared with well-known published experimental results, the results are found to be in an excellent agreement. Effect of main dimensionless parameters such as compressor length/compressor diameter and flow velocity are considered. It is found that the increasing the velocity parameter up to two the surge will change from classical surge into the deep surge. Also, the increase of the compressor dimensionless length up to 8 will cause the surge and rotating stall to reach the stable condition faster than the cause when it is equal to 4. Also, it is important to notice that Fehlberg method predicted the surge and rotating stall much closer to the Runge Kutta fourth degree method by about 7%.

Keywords- Stall and surge, axial Compressor, Numerical Solution, Runge Kutta method, Fehlberg Method.

1. INTRODUCTION

The major purpose of the present work is to identify the physics of axial compressor stall and surge, to develop a suitable numerical method to prevent these instabilities. Through this study of the rotating stall and surge theory and the laboratory experiments developed by the Moore-Greitzer model and considering several numerical methods to minimize the effect of surge and the rotating stall phenomena. Most of the compressor systems are currently designed using numerical solutions to reduce or limit the extent of these phenomena. The properties of compressor instability were discussed by Greitzer [1]. Greitzer describes in details his experimental

study for the axial flow compressor surge and rotating stall. The experiments are conducted using a 3-stage axial compressor. With his experimental setup, Greitzer varied the physical variables of the compression system independently so that their effect on the transient system performance can be observed. Moreover, Greitzer developed a new data evaluation process. He employed the concept of the plenum mass equilibrium. These concepts make it able to direct computing compressor mass flow accurately.

Day et al. [2] present a correlation for estimating the characteristics performance of multi-stage and single-stage axial compressors in rotating stall. They derived the relationship from new stalled

compressor performance set up. The new measurements had been carried out using several different compressor configurations. Day et al [2] also, varied the compressor design parameters systematically to see the influence of each parameter. Mazzawy [3] has pointed out in his work the important discussion about the mechanics of the surge phenomenon and its important on engine design. His work proposes a quite simple models for estimating surge induced loads on various engine elements. The basis for these models was an empirical correlation of surge induced inlet over pressure based on engine pressure ratio and bypass ratio. He derived an approximate estimate of the post-surge axial pressure distribution from that correlation by assuming that surge initiation occurs in the rear of the compression system. Stenning [4] reported some simple criteria for determining system stability. Also, Stenning [4] dividing the multistage compressor into several stream tubes and computing rotating stall criteria for each tube and blade row, and found that surge occurs when the stream tube close to the hub was unstable for rotating stall. A one-dimensional model was presented by Sugiyama et al. [5] for simulating surge disturbance propagations throughout an entire turbojet engine. The predicted results using this model were presented for the surge transient flow phenomena and the unsteady compressor operating point excursion during a surge in a J8S-Turbojet engine. The measurements details for a low speed air compressor test equipment instrumented to understand the details of axial flow and circumferential flow disturbances is presented by Day [6] measurement results showed that compressor air surge was started by air compressor rotating stall and that the resulting air surge cycle was a sequence of well consistent of both cause-and-effect event. The differences in air cycle behaviour between classic air surge and deep air surge were investigated, and it was demonstrated that the shape of the compressor characteristic behaviour determines which of these events occurrences. From these results, it also was noticed that some important parameters, such overall pressure rise and size of hysteresis loop, which was not received enough attention in existing methods for predicting the rotating stall/surge limits.

Young-Jin Jung et al. [7], they showed that the stall cell blockage was an important parameter for correlating the flow regimes in stall, and hence the overall compressor performance. The

resulting correlation, which they developed, was based on a heuristic model of the stalled flow that can be applied whether a given compressor will exhibit full-span or part-span stall, as well as the extent of the stall-unstall hysteresis loop. He found a different stall method to result in different compressor operating point excursions. Mohsen [8], improved the overall performance of the compressors by evaluating the compressor fundamental stall and surge parameters. It may also be shown when the angle of the feather is adjusted increases the angle of airflow occurrence and increases the dynamic load antenna. Tianyu Pan et al. [9] represented the unknown stalled compressor stage characteristics by parameters (pressure rise, mass flow, time constant and efficiency) whose range was determined through a parametric study. The predicted stalled characteristics showed faster response and larger pressure ratio deterioration compared to low speed compressors. Based on the comparison of the circumferential velocity between the numerical and the theoretical results, it was found that the rim of the recessed blade tip can work as the labyrinth seal and consequently reduce the mass flow rate through the tip clearance and found that Surge hammer overpressures had a triangular shape in the time Space (engine axis) domain. Also, found that the mass flow through is approaching zero in 10-20 mms, thus affecting the peak hammer over pressures at the intake duct and the temperature rise in the compressor. Compressor performance was significantly improved by 17%.

Munari et al.[10] reported that the compressor system performance was coupled to the unsteady pressure measurements to provide the first detailed quantitative picture of instantaneous compressor operation during both compressor air surge and air compressor rotating stall transients. He compared the experimental results to a theoretical model of the transient system response.

Different types of compressor instability were studied thoroughly by Xiang Xue et al. [11] identified and their effect on the operating point has been analyzed and discussed the effects of different rotary angles on the shift from the stall to the surge within the blades of the compressor. The theoretical criterion for predicting the mode of compression system instability, rotating stall and surge, was found in good agreement with the data. Mauro Righi et al.

[12] the model was designed for a three-phase, low-speed three-phase axial compressor in all operating zones. It was found that the size of the reservoir after the compressor affected the type of instability and thus affected the stall and surge. It was shown that the model provides adequate quantitative description of the motion of the compression system operating point during the transients that occur subsequent to the onset of axial compressor stall. Therefore, the present work is aimed at investigating the effect of two dimensionless parameters first is the compressor length divided by the compressor diameter and dimensionless velocity parameters on the compressor stability.

Preliminaries

The well-known model of Moore-Greitzer will be analyzed in this work and a diagrammatic sketch for this model shown in Figure 1. This model will be referred to as the compression system. It comprises of a discharging tube to a downstream plenum room. These plenum sizes are big compared to those of the compressor and its tubes. So that it is considered to have negligible the velocities of the fluid and their derivatives in the plenum.

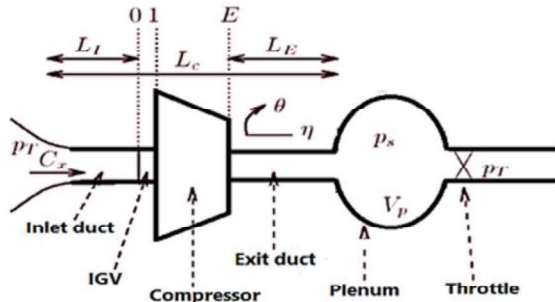


Fig 1 Typical Diagrammatic Sketch for Compressor System

Modeling Compressor:

According to Gravdahl [13], all distances are non-dimensional by average axial compressor half diameter R . The non-dimensional circumferential coordinate is then simply the impeller angle, θ while the axial distance, also referred to R , is designated by ξ and time is designated by half the diameter of impeller moved as:

$$\xi = \frac{Ut}{R} \quad (1)$$

The increase of pressure above a single blade row is:

$$\frac{\Delta p}{\frac{1}{2}\rho U^2} = F(\phi) - \tau \frac{d\phi}{dt} \quad (2)$$

Where $\phi = \frac{C_x}{U}$ is the axial local flow coefficient

$$\left(\frac{d\phi}{dt}\right)_{stator} = \frac{U}{R} \frac{\partial \phi}{\partial \xi} \quad (3)$$

$$\left(\frac{d\phi}{dt}\right)_{rotor} = \frac{U}{R} \left(\frac{\partial \phi}{\partial \xi} + \frac{\partial \phi}{\partial \theta}\right) \quad (4)$$

Where Φ is the coefficient of axial flow at the annulus mean, Ψ is the total to static rise coefficient, J is the square of the amplitude.

For a compressor of N stages

$$\frac{P_E - P_1}{\rho U^2} = NF(\phi) - \frac{1}{2a} \left(2 \frac{\partial \phi}{\partial \xi} + \frac{\partial \phi}{\partial \theta}\right) \quad (5)$$

Where:

$$a = R / N \tau U \quad (6)$$

It is noticed that the coefficient of flow ϕ can depend on both θ and ξ however the Atmospheric total (stagnation) Pressure P_T is constant. The mean of ϕ around the wheel is defined as:

$$\frac{1}{2\pi} \int_0^{2\pi} \phi(\xi, \theta) d\theta \cong \Phi(\xi) \quad (7)$$

Further

$$\phi = \Phi(\xi) + g(\xi, \theta), h = h(\xi, \theta) \quad (8)$$

Where h is a circumferential coefficient of velocity. As no circulation happens in the entrance pipe the means of g and h vanish:

$$\int_0^{2\pi} g(\xi, \theta) d\theta = 0; \int_0^{2\pi} h(\xi, \theta) d\theta = 0 \quad (9)$$

Entrance pipe and inlet guide vanes (IGV)

The difference in pressure over the IGV, Where the flow is axial, can be written

$$\frac{P_1 - P_0}{\rho U^2} = \frac{1}{2} K_G h^2 \quad (10)$$

Where $0 < K_G \leq 1$ is the coefficient of entrance recovery so, the IGV is lossless so, $K_G = 1$

.So, the irrational flow upstream of the IGV is considered unsteady; so, the velocity potential

Occurs. The velocity gradient of $\bar{\phi}$ gives axial and circumferential coefficient of velocity's.

However, at the entrance pipe, i.e. at the IGV entrance fluid properties (denoted by subscript '0') then:

$$(\bar{\phi}_\eta)_0 = \Phi(\xi) + g(\xi, \theta) \text{ and } (\bar{\phi}_\theta)_0 = h(\xi, \theta) \quad (11)$$

Where partial differentiation with respect to η and θ is designated by subscripts. Equation of Bernoulli for unsteady without friction and non-compressible flow will be considered to estimate the entrance pressure drop in the pipe. As reported by J. Gravdahl [13] this will be given as:

$$\frac{p_T - p_o}{\rho U^2} = \frac{1}{2}(\phi^2 + h^2) + (\bar{\phi}_\xi)_o \quad (12)$$

Where the parameter $(\bar{\phi}_\xi)_o$, is the unsteadiness in Φ and g . A straight inlet pipe of dimensionless length l_1 , is considered, and the velocity potential can be given by:

$$\bar{\phi} = (\eta + l_1)\Phi(\xi) + \bar{\phi}'(\xi, \eta) \quad (13)$$

Where $(\bar{\phi}')$ is the term due to the disturbance velocity potential tending to zero at $\eta = -l_1$ and can be written in g and h at a point 0 as:

$$(\bar{\phi}')_o = h(\xi + \theta) \quad (\bar{\phi}'_\eta)_o = g(\xi, \theta) \quad (14)$$

Then equation (12) is now given by:

$$\frac{p_T - p_o}{\rho U^2} = \frac{1}{2}(\phi^2 + h^2) + l_1 \frac{d\Phi}{d\xi} (\bar{\phi}_\xi)_o \quad (15)$$

Exit pipe and guide vanes:

The exit compressor flow is complex and rotating. As in F. K. Moore [14], the pressure P at the pipe exit is assumed only to be vary fairly from the static pressure of the plenum, $p_s(\xi)$, in the way that the coefficient of pressure P satisfies Laplace's equation.

$$P \equiv \frac{p_s(\xi) - p}{\rho U} \quad (16)$$

The axial flow Euler equation is given in J. Gravdahl [13]. It considered to estimate the pressuredrop through the exit pipe.

$$(p_\eta)_E = (\bar{\phi}_{\eta\xi})_o = \frac{d\Phi}{d\xi} + (\bar{\phi}'_{\eta\xi})_o \quad (17)$$

At $\eta = l_g$ (pipe exit), $p = p_s(\xi)$, $P = 0$

.Thus, integrating Eq. (17) leads to:

$$P = (\eta - l_g) \frac{d\Phi}{d\xi} - \bar{\phi}'_\xi \quad (18)$$

Finally

$$\frac{p_s - p_E}{\rho U^2} = (P)_E = -l_E \frac{d\Phi}{d\xi} - (m - 1)(\bar{\phi}'_\xi)_o \quad (19)$$

Where m is the compressor pipe flow parameter (m = 2 refer to long enough exit pipe and m=1 refer to very short one).

Total pressure balance

From the previous relations, we can obtain a relation for the final pressure increase from the reservoir upstream (atmosphere) stagnant pressure P_T to static the plenum pressure P_S at the exit Flow of the outlet pipe. This is carried out by adding equations (5, 10, 15 and 19) and considering ($K_G = 1$) the net equation is:

$$\Psi(\xi) = \psi_c(\phi) - l_c \frac{d\Phi}{d\xi} - m(\bar{\phi}'_\xi) - \frac{1}{2}(2\bar{\phi}'_{\xi\eta})_o \quad (20)$$

Where:

$$\Psi(\xi) \equiv \frac{p_s - p_T}{\rho U^2}$$

$$\psi_c(\phi) \equiv NF(\phi) - \frac{1}{2}\phi^2$$

$$l_c \equiv l_1 + \frac{1}{2} + l_E$$

$$\phi = \Phi + (\bar{\phi}'_\eta)_o$$

The potential velocity disturbance $\bar{\phi}'$, that satisfies Laplace's equation which its solution is a Fourier series solution. Then using one term of this series as in J. Gravdahl [13] find that

$$(\bar{\phi}'_\eta)_o = -(\bar{\phi}'_{\theta\theta})_o \quad (21)$$

And

$$(\bar{\phi}'_\eta)_o = -(\bar{\phi}'_{\theta\theta})_o \quad (22)$$

Substitute in Equation (20) the result is

$$\Psi(\xi) = \psi_c(\Phi - Y_{\theta\theta}) - l_c \frac{d\Phi}{d\xi} - mY_\xi + \frac{1}{2a}(2Y_{\xi\theta\theta} + Y_{\theta\theta\theta})_o \quad (23)$$

Plenum mass balance:

The plenum mass balance given by J. Gravidahl [5], is:

$$l_c \frac{d\Psi}{d\xi} = \frac{1}{4B^2} [\Phi(\xi) - \Phi_T(\xi)] \quad (24)$$

$$B \equiv \frac{U}{2a} \sqrt{\frac{V_P}{A_C L_C}} \quad (25)$$

Where V_P is the compressor plenum volume, A_C is the compressor inlet area, and L_C is compressor total length and a_s is the speed of sound. The characteristics of the compression system are like those of Moore [14].

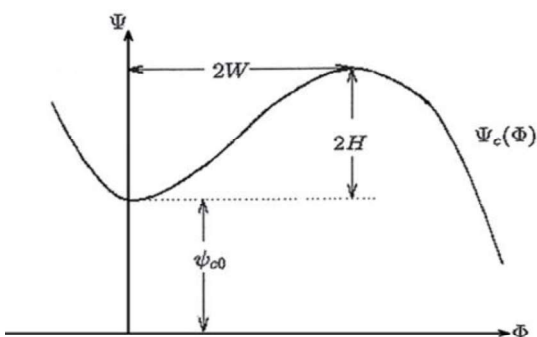


Fig 2: Typical Cubic Compressor Characteristic

$$\Psi_c(\phi) = \psi_{c0} + H \left[1 + \frac{3}{2} \left(\frac{\phi}{W} - 1 \right) - \frac{1}{2} \left(\frac{\phi}{W} - 1 \right)^3 \right] \quad (26)$$

Where the terms ψ_{c0} , H and W are shown in figure 2. The compressor throttle characteristic

$$\text{Is: } \Psi(\xi) = \frac{1}{2} K_T \Phi_T^2 \quad (27)$$

There are only two equations for the three unknowns: $\Psi(\xi)$, $\Phi(\xi)$ and $Y(\xi, \theta)$ the third Equation comes from taking the mean of Equation (22) over the Annulus, the result is:

$$\Psi(\xi) + l_c \frac{d\Phi}{d\xi} = \frac{1}{2\pi} \int_0^{2\pi} \Psi_c(\Phi - Y_{\theta}) d\theta \quad (28)$$

Final model:

As J. Gravidahl [13] suggested to use Galerkin procedure to alter the partial differential equation(22) to ordinary differential Equation by using a first Harmonic function of (Y).

$$Y = WA(\xi) \sin(\theta - r(\xi)) \quad (29)$$

Where $A(\xi)$ is amplitude and $r(\xi)$ is the phase angle, the finale model becomes:

$$\frac{d\Psi}{d\xi} = \frac{W}{4B^2} \left[\frac{\Phi}{W} - \frac{\Phi_T}{W} \right] \frac{H}{l_c} \quad (30)$$

$$\frac{d\Phi}{d\xi} = \left[-\frac{\Psi - \psi_{c0}}{H} + 1 + \frac{3}{2} \left(\frac{\Phi}{W} - 1 \right) - \frac{1}{2} \left(\frac{\Phi}{W} - 1 \right)^3 \right] \frac{H}{l_c} \quad (31)$$

$$\frac{dJ}{d\xi} = J \left[1 - \left(\frac{\Phi}{W} - 1 \right)^2 - \frac{1}{4} J \right] \frac{3aH}{(1+ma)W} \quad (32)$$

Where $J(\xi) = A^2(\xi)$

The results of the experiment were given in J. Gravidahl [13] and the relationship between ζ

(Dimensionless) on the axis of x and Φ (Dimensionless) on the axis of the relationship between ϕ the dimensionless axial compressor flow coefficient and ζ dimensionless time Coefficient.

Table 1 Numerical Values employed in the computer code for the two models.

Symbols	Value	Symbols	Value
H	0.18	K_T	5.5
W	0.25	B	0.5,1.0,2.0
m	1.75	l_c	8.0,6.0,4.0
ψ_{c0}	0.3	J	0.0004

Numerical Model Validation

Comparison between experimental results and numerical method

All the numerical values for the parameters in the models are given in Table 1, The initial values of the non-dimensional pressure rise Ψ_0 and flow coefficient Φ_0 are considered to be the values at the tip of The compressor characteristic curve which are $\Psi_0 = 0.66$, $\Phi_0 = 0.5$ for the particular compressor Characteristic chosen two cases are considered for comparison. The comparison is carried out with data Of J. Gravidahl [13]. Calculated for compression system flow without inlet distortion $\varepsilon = 0$. The Operating condition case shows that the compression system transient behavior in surge and stall, be done in two ways, the Runge Kutta method Steven C. Chapra [15] and Runge Kutta Fehlberg method F. Gerald, O. Wheatley [16].

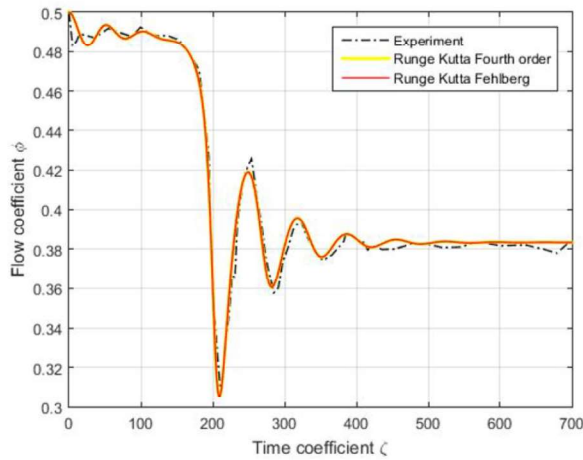


Fig 3: Comparison between Experiment, Runge Kutta method, and Fehlberg method(Present Work) at $B=0.5$

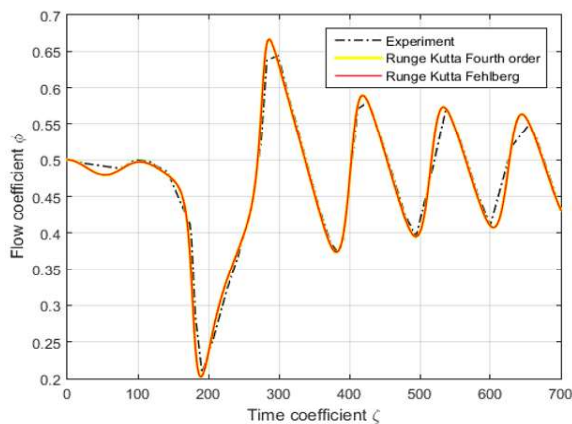


Fig 4: Comparison between Experiment Results, and Runge Kutta Method, and Fehlberg Method (Present Work) at $B=1.0$

A Program was designed by MATLAB and codes were made for the two methods and compared to the experiment of Gravdahl [13] to ensure the success of the program. The maximum difference between the two methods is found not to exceed 7%. A Comparison is made with Gravdahl [13] for two Situations of transient behavior system one is the rotating Stall and the other one is for the surge.

In solving the problem, three values for B are considered.

The results are presented in Figure 3 with the value of $B = 0.5$, this Figure 3 indicates excellent agreement between the two results for the two methods (surge and stall). The Method Runge Kutta Fehlberg is more precision than the Runge Kutta Method When $B = 0.5$ as seen in Figure 3. The stall cycle can be seen when the system reaches the throttle curve with new operation point. The flow and pressure coefficients, ϕ & ψ reach to the steady state at approximately time (ζ) = 500 as shown in Figure 3.

When $B = 1.0$, as in Gravdahl [13] oscillations will always be as in Figure. 4 And there will be no damping and we will also make a comparison in this case. The Runge Kutta Fehlberg method is more precision than the Runge Kutta 4th order method When $B = 1.0$ as shown in figure 4. the system entering to classic surge cycle as shown in this figure, the flow and pressure coefficient ϕ starts to oscillate and do not reach steady state values.

Present Work Results

Effect of Velocity Parameter (B)

The effect of velocity parameter B on the compression system transient behavior and compression system characteristic without inlet distortion are investigated in this section. The geometrical, operation conditions and inlet distortion parameters are kept to their values as described in the previous section, While, the parameter B is changed from the value of 0.5, 1.0 and 2.0. The results are plotted in Figure 5 to Figure 13. These figures -indicate that the higher value of B causes large excursions in axial flow coefficient ϕ . At the highest value of B , this would lead to surge cycles, whereas for the lower values, the system operates at stall cycles.

When $B = 0.5$ as shown in Figure 5, the stall cycle can be seen when the system reaches the throttle curve with new operation point. The flow and pressure coefficients, ϕ and ψ reach to the steady state in time about $\zeta = 500$ as shown in figures 5, 6. The stall amplitude J , as shown in figure 7, starts to increase and oscillate until it reaches to steady state at the value of $J=2.86$ in time about $\zeta = 470$.

At $B = 1.0$ the system entering to classic surge cycle as shown in Figures 8 , 9 The flow and pressure coefficients, ϕ & ψ , as shown in figure start to oscillate and do not reach to steady state values. Also, it can be shown that from figure 10, the amplitude of stall J starts to increase and decrease then reaches to steady state at very low value almost zero (no stall) in time about $\zeta = 290$.

Finally, when $B = 2.0$ the system operates under deep surge cycle as can be shown in figures the deep surge cycle with back flow phenomena (reverse flow) is found. Also, figures 11, 12 show the oscillation of the flow and pressure coefficients ϕ and ψ . They start to oscillate in high amplitude and do not reach to steady state. The amplitude in figure 13 of stall J again reaches to steady state at very low value (no stall) in time about $\zeta = 190$.

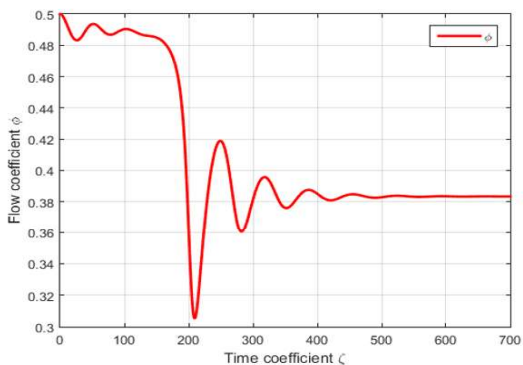


Fig 5: Transient average flow coefficient at B=0.5

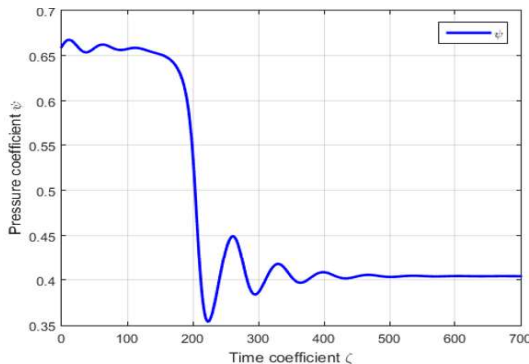


Fig 6: Transient average pressure coefficient at B=0.5

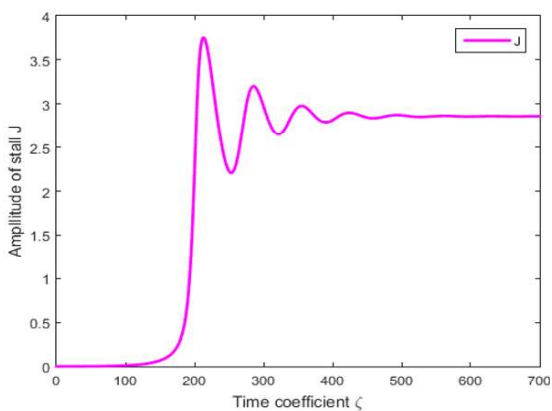


Figure 7: Transient amplitude of stall at B=0.5

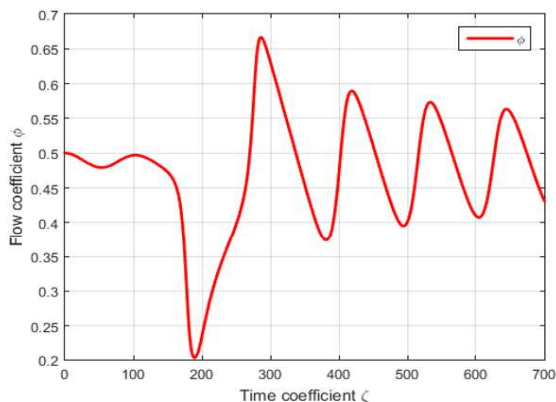


Fig 8: Transient average flow coefficient at B=1.0

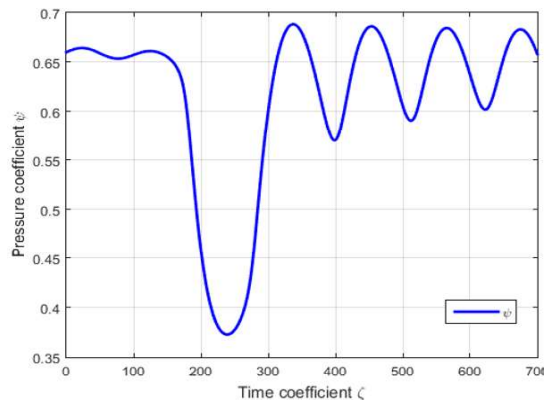


Fig 9: Transient average pressure coefficient at B=1.0

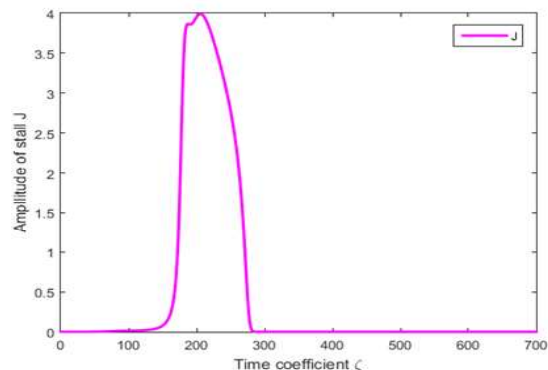


Fig 10: Transient amplitude of stall at B=1.0

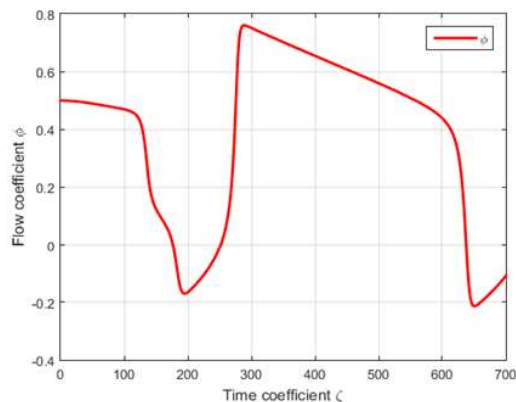


Fig 11: Transient average flow coefficient at B=2.0

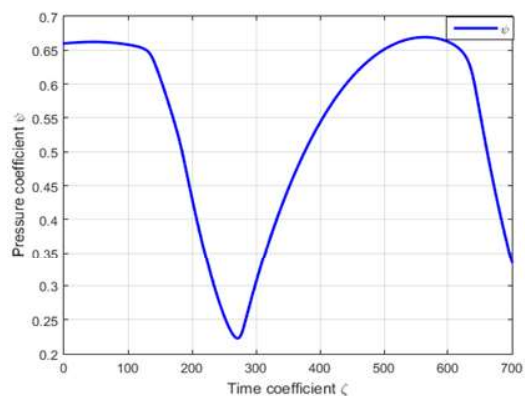


Fig 12: Transient average pressure coefficient at B=2.0

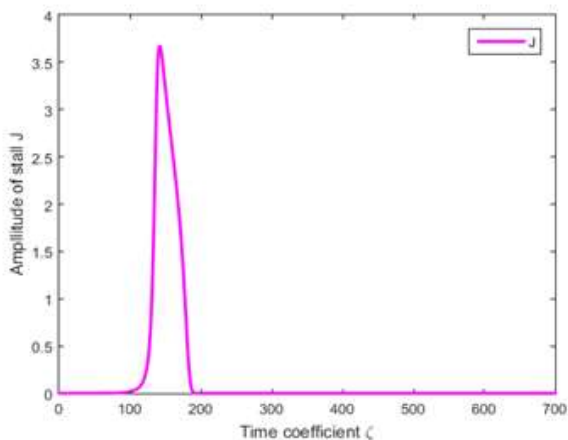


Fig 13: Transient amplitude of stall at B=2.0

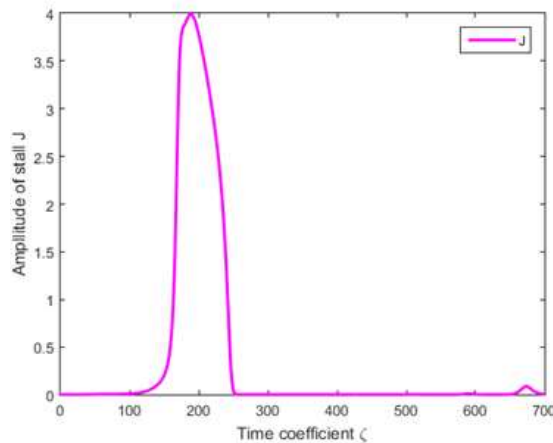


Fig 15: Transient amplitude of stall at B=1.0 ,
 $l_c = 6.0$

Effect of Compressor Length

The other parameter investigated is a compressor length l_c Figures 14, 15 and 16 show trajectories for the amplitude of stall at three different values of l_c equal to 8.0, 6.0 and 4.0. While value of B is to be 1.0 and the initial amplitude of stall is $J=0.0004$ and $\epsilon=0.0$ (no distortion). The curves for $l_c=8.0$ and 6.0, while quantitatively is different, they have the same qualitative features, namely an initial rapid rise in amplitude and then reach to the steady state. A different situation exists for $l_c=4.0$ Where the

amplitude of stall starts to oscillation and never reach to steady state which leads the compression system

to enter to combined cycle from the classic surge and rotating stall which known as modified surge. The reason for this physical behaviour is that the value of B reduces in length will produce a relatively rotating stall cell time formation is longer in proportional to the time for a mass flow excursion.

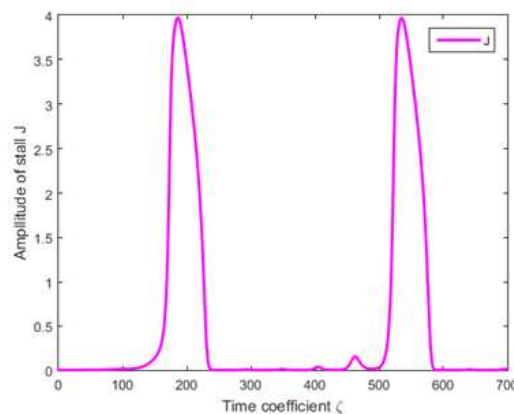


Fig 15: Transient amplitude of stall at B=1.0 ,
 $l_c = 4.0$

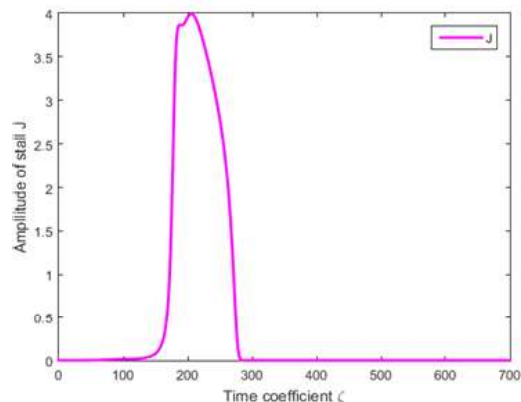


Fig 14: Transient amplitude of stall at B=1.0 ,
 $l_c = 8.0$

Conclusion

The used model developed for the simulation of axial flow compression system to investigate the behaviour through the unstable region of surge and rotating stall by employing two numerical methods.

- 1) The results show that the higher values of velocity parameter B will cause large excursions in axial flow coefficient ϕ . This would lead the system to surge cycles however, its lower values the system operates at rotating stall cycles. The other effect of this parameter is on the amplitude of stall where it decays for large values of B and evolves at a fixed level when B is less than critical values.
- 2) The compressor length parameter also has strong effects on the system. The present study shows that, for a given value of velocity parameter B, compressors of shorter length entering to modified surge cycle.
- 3) The effects of the initial condition of the stall amplitude J appears only on the amplitude of the stall transient behavior. By increasing of the

initial condition of stall the time which the amplitude of stall takes, to reach to steady state is decreasing.

4) The effects of inlet distortion on compression system behavior were studied for two situations:

a) When the system in 'rotating stall, the small value of amplitude of inlet distortion

Makes no change in general behavior of the compression system. By increasing the

Value of amplitude of inlet distortion, the compression system entering to modified

Surge cycle.

b) When the system in classic surge cycle, any value of amplitude of inlet distortion

Leads the system to modified surge cycle.

The following recommendations are suggested for further studies:

1) Extend the model by regarding the complete gas turbine assembly which includes Air intake-compressor-turbine-jet nozzle system.

2) Effect of heat addition and pressure drop in the burner.

3) Evaluation of the available surge-rotating stalls control system with consideration

Of the achieved results.

Nomenclature

A Amplitude function of rotating stall (dimensionless)

A_C Compressor duct area (m^2)

a Reciprocal time lag parameter of blade passage (dimensionless)

a_s Sound Speed A (m / sec)

B Parameter
$$B = \left(\frac{U}{2a_s} \right) \sqrt{\frac{V_p}{A_c L_c}}$$
 (dimensionless)

C_x Velocity Components along Compressor axis (m / sec)

F Pressure rise coefficient in blade passage (dimensionless)

g Disturbance in axial flow coefficient (dimensionless)

H Semi height of cubic axisymmetric characteristic (dimensionless)

h Circumferential velocity coefficient (dimensionless)

J Square of Amplitude = A^2 (dimensionless)

K_G Loss coefficient at inlet guide vanes (IGV) (dimensionless)

K_T Throttle coefficient (dimensionless)

l_C Aerodynamic length of compressor L_C / R (dimensionless)

l_E, l_I, l_T Length of exit, Entrance, and throttle duct $L_E / R, L_I / R, L_T / R$

m Compressor duct flow Parameter (dimensionless)

N Number of stages of Compressor

P Pressure Coefficient (dimensionless)

P_o Static pressure at entrance to (IGV) (N / m^2)

P_I, P_E Static Pressure at entrance and exit of compressor (N / m^2)

P_S Pressure in the plenum (N / m^2)

P_T Total pressure ahead of entrance and following the throttle duct

R Mean wheel radius (m)

r Phase angle (radial)

t Time (second)

U Wheel speed at mean diameter (m / sec)

V_p Volume of plenum (m^3)

W Semi width of cubic characteristic (dimensionless)

Y Disturbance potential at compressor entrance (dimensionless)

η Axial distance = x / R (dimensionless)

θ Angular coordinate around wheel (radial)

- ξ Nondimensional time $\xi = \frac{Ut}{R}$
(dimensionless).
- ρ Density (Kg / m^3)
- τ Coefficient of pressure rise lag (Second)
- Φ Annulus average axial flow coefficient
(dimensionless)
- Φ_T Flow coefficient of throttle duct
(dimensionless)
- ϕ Local axial flow coefficient $\phi = \frac{C_x}{U}$
(dimensionless)
- $\bar{\phi}$ Velocity potential in entrance duct
(dimensionless)
- $\bar{\phi}^{\wedge}$ Disturbance velocity potential
(dimensionless)
- Ψ Total static pressure rise coefficient
(dimensionless)
- ψ_C Axisymmetric pressure rise coefficient
(dimensionless)
- ψ_{CO} Shut of value of axisymmetric coefficient
(dimensionless)
- ε Amplitude of velocity distortion
(dimensionless)

References

- [1] E. M. Gritzer, surge and rotating stall in axial flow compressors, Parts I, II, ASME journal of engineering for power, Vol. 98, 1976, PP 192-21.
- [2] I. J. Day, N. A. Cumpsty and E. M. Gritzer, Prediction of compressor performance in rotating stall, ASME journal of engineering for Power, Vol. 100, 1978, PP 1-12.
- [3] R. S. Mazzawy, Surge- Induced structural loads in gas turbines, ASME journal of engineering for power, Vol. 102, 1980, PP 162-168.
- [4] F. K. Moore, a Theory of rotating stall of multistage axial compressors, Parts I, II, III, ASME journal of engineering for power, Vol. 106, 1985, PP 313-336.
- [5] Y. Sugiyama, W. Tabakoff and A. Hamed, J85 Surge transient simulation, journal of propulsion and power, Vol. 5. No 3, 1989, PP 375-381.
- [6] I. J. Day, Axial Compressor performance during surge, journal of propulsion and power, Vol. 10. No 3, 1994, PP 329-337.
- [7] Young-Jin Jung, Heungsu Jeon, Yohan Jung, Kyu-Jin Lee and Minsuk Choia, Effects of recessed blade tips on stall margin in a transonic axial compressor. Volume 54, 2016, Pages 41-48.
- [8] Mohamed Mohsen, Farouk M. Owis, Ali A. Hashim. The impact of tandem rotor blades on the performance of transonic axial compressors. Volume 67, 2017, Pages 237-248.
- [9] Tianyu Pan, Qiushi Li, Wei Yuan and Hanan Lu, Effects of axisymmetric arc-shaped slot casing treatment on partial surge initiated instability in a transonic axial flow compressor. Volume 69, 2017, Pages 257-268
- [10] E. Munari, M. Morini, M. Pinelli, P.R. Spina, A. Suman. Experimental investigation of stall and surge in a multistage compressor. J Eng Gas Turbopower, 139 (2) (2017), p.022605
- [11] Xiang XUE, Tong WANG, Tongtong ZHANG, Bo YANG, Mechanism of stall and surge in a centrifugal compressor with a variable vaned diffuser, Chinese journal of aeronautics, Volume 31, Issue 6, 2018, Pages 1222-1231.
- [12] Mauro Righi, Vassilios Pachidis, László Könözsy, Lucas Pawsey, Three-dimensional through flow modelling of axial flow compressor rotating stall and surge. Volume 78, 2018, Pages 271-279
- [13] J. Gravdahl, Modeling and control of surge and rotating stall in compressors, Ph. D., Thesis, department of engineering cybernetics Norwegian University of science and technology, 1998.
- [14] F. K. Moore, a Theory of rotating stall of multistage axial compressors, Parts I, II, III, ASME journal of engineering for power, Vol. 106, 1985, PP 313-336.
- [15] Steven C. Chapra, Raymond P. Canale Numerical methods for engineering, sixth edition 1996.
- [16] F. Gerald, O. Wheatley, Applied Numerical analysis, Adeson-Wesley, fifth edition, 1994.